

# A new Monte Carlo method to study the fluid-solid phase transition of polydisperse hard spheres

Mingcheng Yang and Hongru Ma\*

*Institute of Theoretical Physics, Shanghai Jiao Tong University,*

*Shanghai 200240, People's Republic of China*

(Dated: November 12, 2018)

## Abstract

A new Monte Carlo approach is proposed to investigate the fluid-solid phase transition of the polydisperse system. By using the extended ensemble, a reversible path was constructed to link the monodisperse and corresponding polydisperse system. Once the fluid-solid coexistence point of the monodisperse system is known, the fluid-solid coexistence point of the polydisperse system can be obtained from the simulation. The validity of the method is checked by the simulation of the fluid-solid phase transition of a size-polydisperse hard sphere colloid. The results are in agreement with the previous studies.

PACS numbers: 05.10.Ln, 62.20.Dc, 82.70.Dd

---

\*Electronic address: hrma@sjtu.edu.cn

Melting and freezing transitions are among the most important phenomena in condensed matter physics. The determination of the equilibrium phase diagram of a specific material is the key point in the understanding of the equilibrium properties of the material. The hard sphere system(HSS), which is a representative model of a large class of colloidal suspensions, has been extensively investigated. It is well known that HSS undergoes an entropy driven first-order phase transition from a disordered fluid to an ordered solid as the packing fraction increases [1]. However, in a true colloidal system the particles are inevitably polydisperse in particle sizes, which can be measured by the ratio of the standard deviation to the mean of the diameter,  $\delta = \frac{\sqrt{(\sigma-\bar{\sigma})^2}}{\bar{\sigma}}$ . It has a remarkable effect on the thermodynamic and dynamic behaviors of the HSS [2, 3, 4, 5, 6, 7]. The influence of the polydispersity on the fluid-solid phase transition of the HSS has been studied experimentally [2], and theoretically by computer simulation [3], density functional theory [8, 9], moment free energy method [4] and other simplified theories [10, 11, 12]. Experimentally, crystallization process depends on the nonequilibrium effects [13, 14], as a result the observed phase behaviors deviate more or less from the equilibrium case. However, the theoretically obtained phase diagram is usually the equilibrium one. Therefore, the simulation study of freezing transition of the polydisperse HSS is essential to check the validity of the theory and to deeply understand the equilibrium phase behaviors of the system.

When studying the fluid-solid coexistence of the polydisperse HSS by computer simulations, there exist two basic difficulties which also exist in the monodisperse case: one is that the coexisting solid forbids the particle insertion; and the other is that the back and forth tunneling event between the liquid and solid phases never happens within the simulation time scale. Therefore, some usual methods, by which the phase transition of the polydisperse soft spheres [15, 16] and the nematic-isotropic transition of polydisperse liquid crystal [17] can be investigated effectively, are not suitable for the problem. To the best of our knowledge, Gibbs-Duhem integration algrithm[3] is the only available assumption-free method to determine the phase behavior of polydisperse HSS, where the coexistence curve is obtained by integrating the Clausius-Clapeyron equation from the monodisperse hard sphere coexistence states. However, the method is not very robust and lacks built-in diagnostics, and no other simulation data are available for comparison. Thus it is desirable to develop such an approach by which the phase transition can be determined from the rigorous free energy calculation. One possible scheme is to directly estimate the free energy difference

between the stable polydisperse hard sphere fluid and solid phases. In principle, the semi-grand ensemble lattice switch method [18, 19] is a feasible one. However, the implementation of a simulation along this line is nontrivial. First, the free energy difference between the fluid and the solid phases is huge, second, the system need to traverse a enormous entropy barrier(“gate” state), and third, the symmetry of fluid phase is not the same as solid phase. The other possible scheme is the so called referenced-state method [20, 21]. For the polydisperse HSS the best reference states are just the coexisting fluid and solid of monodisperse HSS. Unfortunately, in the simulation it is often difficult to find a reversible path linking the monodisperse reference state to the polydisperse system under consideration. The reason is that the ensemble for simulating the polydisperse system(semigrand ensemble) is different from that for the monodisperse system(canonical ensemble).

In the present work, we use the concept of extended ensemble to construct a reversible path connecting the polydisperse target state to the monodisperse reference state, along which the free energy difference between polydisperse and monodisperse system can be estimated easily. By the method we reinvestigate the fluid-solid phase transition of polydisperse HSS.

The semigrand canonical ensemble (SCE) is the best frame to investigate the phase behavior of a polydisperse HSS. In this ensemble the independent variable is the chemical potential difference function, the total number of particles is fixed and the number of particles of each size is permitted to fluctuate. A continuous composition distribution can be realized on average. Generally the composition distribution can not be prescribed in advance unless we know the conjugated chemical potential difference function. Fortunately, the chemical potential difference function can easily be obtained by the recently developed SNEPR method, which was described in detail in reference [18, 27]. In all simulation studies of polydisperse systems the polydisperse parameter(diameter of particles here) is always discretized. For the purpose of describing our method more easily, we present the semi-grand canonical ensemble in the case of the discrete diameters. The diameter of particles is assumed to take  $M + 1$  discrete values  $\sigma_i(\Delta) = \sigma_m + (i - \frac{M}{2})\frac{\Delta}{M}$ , here  $i = 0, 1, \dots, M$ ,  $\Delta = \sigma_{max} - \sigma_{min}$ ,  $\sigma_m = (\sigma_{max} + \sigma_{min})/2$ ,  $\sigma_{max}$  and  $\sigma_{min}$  are the maximum and minimum of the allowed diameters of the particles, respectively. In the limit of monodisperse case,  $\sigma_{max} = \sigma_{min} = \sigma_m$ ,  $\Delta = 0$ , and all  $\sigma_i$ ’s are the same. However, we can still regard the particles with different  $i$ ’s as belonging to different species. We will see that this concept is

useful for later construction of reversible paths between a monodisperse and a polydisperse system.

By introducing the excess chemical potential relative to ideal gas  $\mu_{ex}(\sigma_i) = \mu(\sigma_i) - kT \ln(\frac{N\Lambda(\sigma_i)^3}{V})$ , the partition function  $\Upsilon$  for the semigrand canonical ensemble is written as

$$\Upsilon = \frac{1}{N!\Lambda^{3N}(\sigma_r)} \sum_{d_1=\sigma_0}^{\sigma_M} \cdots \sum_{d_N=\sigma_0}^{\sigma_M} Z_N \times \exp \left\{ \beta \sum_{\alpha=1}^N (\mu_{ex}(d_\alpha) - \mu_{ex}(\sigma_r)) \right\}. \quad (1)$$

Here,  $\beta = 1/kT$ ,  $\sigma_r$  is the diameter of an arbitrary chosen referenced component,  $\Lambda(\sigma_r) = h/(2\pi m_r kT)^{1/2}$  is the thermal wavelength of the referenced component,  $d_\alpha$  is the diameter of the  $\alpha$ th particle, and  $Z_N$  is the canonical configuration integral

$$Z_N = \int_{r_1} \cdots \int_{r_N} e^{-\beta U} \prod_{\alpha=1}^N d\mathbf{r}_\alpha. \quad (2)$$

The partition function  $\Upsilon$  is related to the semigrand canonical free energy  $Y$  through

$$Y = -kT \ln \Upsilon(N, V, T, \{\Delta\mu_{ex}(\sigma_i)\}), \quad (3)$$

here  $\Delta\mu_{ex}(\sigma_i) = \mu_{ex}(\sigma_i) - \mu_{ex}(\sigma_r)$ .

In order to establish a reversible path that links the polydisperse system to the monodisperse referenced system, we employ an extended semigrand canonical ensemble in the simulation. In the extended ensemble the range of particle sizes  $\Delta = \sigma_{max} - \sigma_{min}$  is regarded as a new ensemble variable. The extended ensemble is composed of the semigrand canonical ensembles with different range of particle sizes  $\Delta$ . Each value of  $\Delta$  specifies a macroscopic state of the extended ensemble. In what follows, it is convenient to set the diameter of the referenced species  $\sigma_r = \sigma_m$ . With the additional ensemble variable  $\Delta$ , the partition function of the extended semigrand canonical ensemble is defined as

$$\Gamma(N, V, \{\Delta\mu_{ex}(\sigma_i)\}) = \sum_{\{\Delta\}} \Upsilon(N, V, \{\Delta\mu_{ex}(\sigma_i)\}, \Delta), \quad (4)$$

here  $\Delta$  takes a series of discrete values ranged from  $\Delta = 0$  to  $\Delta = \Delta_{max}$ , corresponding to the monodisperse reference system and the polydisperse target system, respectively. The  $\{\Delta\mu_{ex}(\sigma_i)\}$  are kept the same for all values of  $\Delta$ . For  $\Delta = 0$ , the monodisperse case, these  $\{\Delta\mu_{ex}(\sigma_i)\}$  give a distribution of particles among different species with the same diameters, while for  $\Delta = \Delta_{max}$  the  $\{\Delta\mu_{ex}(\sigma_i)\}$  give the required distribution of particles of different sizes. Thus, the monodisperse system can be transformed into the polydisperse

system by the variable  $\Delta$ . For the sake of convenience, the mid-point of the particle sizes,  $\sigma_m = (\sigma_{max} + \sigma_{min})/2$ , is fixed when changing  $\Delta$ . In the simulation the  $\Delta$  moves are performed by resizing all particles, however, the partition of the particles among species remains unchanged even though the particle sizes are changed. The semigrand canonical free energy difference between the macroscopic states  $\Delta = \Delta_{max}$  and  $\Delta = 0$  is written as

$$\Delta Y = \ln \left[ \frac{Pr(0)}{Pr(\Delta_{max})} \right], \quad (5)$$

where  $Pr(\Delta)$  is the probability that the system is in the macroscopic state  $\Delta$ . In the extended semigrand canonical ensemble the probability can be obtained from simulation by the flat histogram methods [24, 25, 26]. In the simulation the trial moves include particle translations, resizing particle operations(breathing move) and changing  $\Delta$  operations.

The semigrand canonical partition function with  $\Delta = 0$  can be written as

$$\Upsilon(N, V, \{\Delta\mu_{ex}(\sigma_i)\}, 0) = \frac{Z_N}{N! \Lambda_m^{3N}} C(N, T, \{\Delta\mu_{ex}(\sigma_i)\}) \quad (6)$$

Where the configuration integral  $Z_N$  is independent of the composition distribution when  $\Delta = 0$ . And  $C(N, T, \{\Delta\mu_{ex}(\sigma_i)\})$  is a summation in the particle species, independent of the volume. Equations (5) and (6) bridge between the semigrand canonical partition function of polydisperse system and the canonical partition function of monodisperse system.

As was well known, the fluid-solid phase transition of monodisperse HSS can be determined by looking for the equal-weight double-peak structure in the volume histogram[22]. In actual computation we use a more tractable criteria “equal peak height” to locate the transition point[23], which differs from equal-weight in the finite-size effect. They give the same result in the thermodynamic limit. If the number of particles of the coexisting fluid is equal to that of the coexisting solid, according to the “equal peak height” condition their canonical partition functions will satisfy the following relation

$$Z_f^c \exp(-\beta P^c V_f^c) = Z_s^c \exp(-\beta P^c V_s^c), \quad (7)$$

here,  $P^c$  is the coexistence pressure,  $V_f^c$  and  $V_s^c$  are, respectively, the volume of the monodisperse coexisting fluid and solid, and  $Z_f^c$  and  $Z_s^c$  are the canonical partition functions of monodisperse coexisting fluid and solid, respectively. Substituting (6) in (7), we get

$$\Upsilon_f(V_f^c, \{\Delta\mu_{ex}(\sigma_i)\}, 0) \exp(-\beta P^c V_f^c) = \Upsilon_s(V_s^c, \{\Delta\mu_{ex}(\sigma_i)\}, 0) \exp(-\beta P^c V_s^c), \quad (8)$$

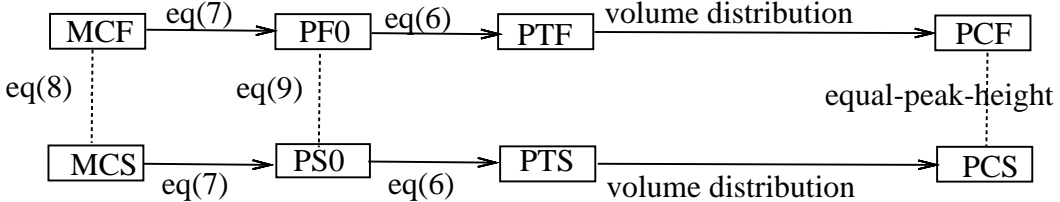


FIG. 1: The flow diagram of the simulation of polydisperse fluid-solid coexistence. The acronym in the small boxes correspond to: MCF and MCS: Monodisperse Coexisting Fluid and Solid; PF0 and PS0: Polydisperse Fluid and Solid with  $\Delta = 0$ ; PTF and PTS: Polydisperse Target Fluid and Solid with  $\Delta = \Delta_{max}$ ; PCF and PCS: Polydisperse target Coexisting Fluid and Solid. The dotted lines describe the coexistence of the fluid and solid phases.

where  $C(N, T, \{\Delta\mu_{ex}(\sigma_i)\})$  is eliminated for it independent of the state of system. Thus, in the polydisperse system with  $\Delta = 0$  the fluid phase is connected to the solid phase. For the polydisperse system with  $\Delta = \Delta_{max}$  that we consider, equations (5) and (8) establish a relation between the fluid phase and the solid phase.

Therefore, once the phase transition point of the monodisperse system is located, combining equations (5) and (8) the semigrand canonical free energy difference between the solid and fluid phases of the polydisperse target system with given  $\Delta_{max}$  and  $\Delta\mu_{ex}(\sigma_i)$  can be calculated by the extended semigrand canonical ensemble simulation where the  $\Delta$  is taken as the ensemble variable. In real calculations the monodisperse coexistence point was taken from literature where the fluid volume fraction is 0.492 and the solid volume fraction is 0.543, respectively. The remaining task to locate the transition point of the polydisperse target system is trivial. The polydisperse target fluid and solid phases are treated as two new referenced states, then the distribution of the volume of the polydisperse target fluid and solid phases can be obtained separately by performing another extended semigrand canonical ensemble simulation, taking the volume  $V$  as the ensemble variable. From such extended ensemble simulations the  $\Upsilon(V)$  can be calculated directly by the flat histogram algorithm. When the volume distribution  $\Upsilon(V)\exp(-\beta PV)$  shows two peaks of equal height, the fluid-solid phases coexistence occurs. The flow diagram of the calculation procedure is shown in figure 1.

To test the validity of our method, we use it to locate the fluid-solid transition point of the polydisperse hard spheres. Our system is composed of 256 size polydisperse hard

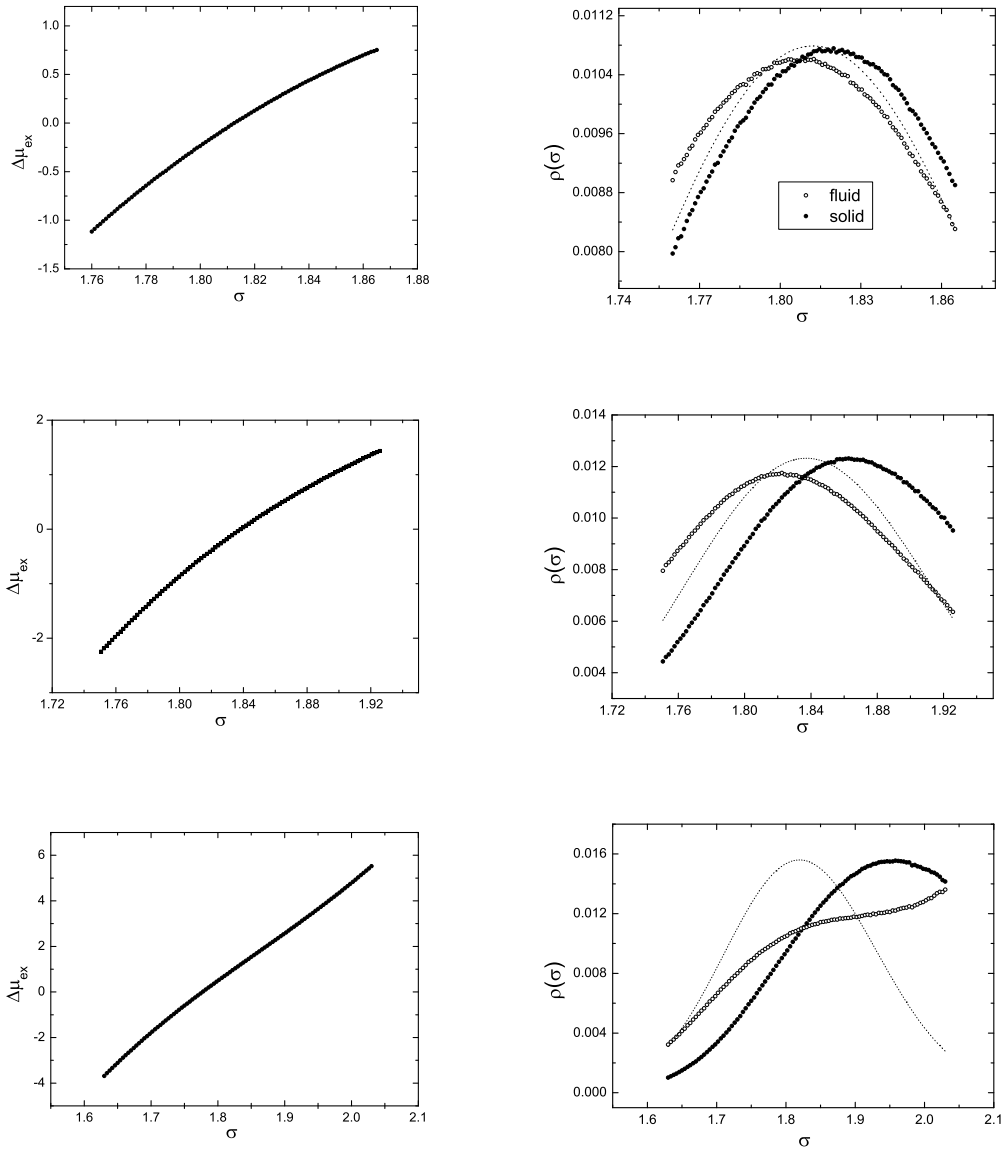


FIG. 2: Left: the chemical potential difference as a function of the particle diameter. Right: the corresponding composition distributions of the coexistence fluid phase(open circles) and solid phase(filled circles). The dotted lines denote the prescribed composition distribution of the initial target polydisperse crystal, here the upper one with a size polydispersity of 0.0163, the middle one with a size polydispersity of 0.0252, and the lower one with a size polydispersity of 0.0507.

spheres contained in a periodic box. The crystal structure under consideration is face-center-cubic (*fcc*), since our previous calculation [18] showed that *fcc* phase is still the most stable structure of polydisperse hard sphere crystal. The composition distribution of the initial target polydisperse solid linked to the referenced monodisperse solid is the truncated

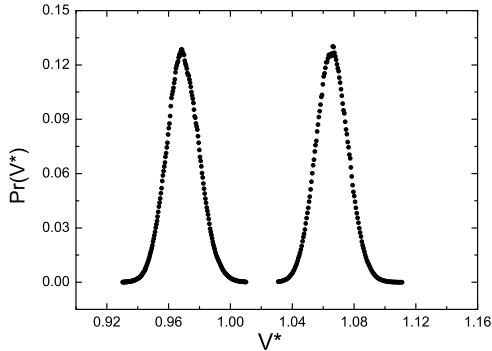


FIG. 3: The probability distribution of the dimensionless volume of the system at coexistence pressure, the imposed chemical potential difference function is the upper one in Fig 2. The dimensionless volume is defined as  $V^* = V/N(\bar{\sigma})^3$ , here  $\bar{\sigma}$  is the average diameter of particles of the initial polydisperse target crystal.

Schultz function. The conjugated chemical potential difference function is evaluated by the SNEPR method. The solved chemical potential difference function is saved and then used to perform the rest of the simulation. The initial target fluid is produced by using the solved chemical potential difference function. Of course, it is possible to prescribe the composition distribution of the initial target fluid rather than the initial target solid. Previous studies by Bolhuis et al used the quadratic form for the chemical potential difference function [3], the corresponding composition distribution is not the same as ours. However, for the same polydispersity  $\delta$  we expect that our simulation will give qualitatively similar results.

Using the SNEPR method we calculated the chemical potential difference functions for three different truncated Schultz distributions in the *fcc* solid phases. Each distribution has different polydispersity, and the maximum one is about  $\delta \simeq 5\%$  because at higher  $\delta$  the crystal may be unstable [2, 3, 4, 9, 28]. Fig.2 shows the chemical potential difference functions and the relevant composition distributions of the coexisting phases. We see that the particle size distribution of the coexisting fluid phase significantly differs from that of the coexistence solid phase, this is the phenomenon named as fractionation, the fractionation effect increases with the polydispersity. Comparing with the coexisting solid, the fluid has larger polydispersity and lower volume fraction. These results are consistent with the previous results [3, 29]. We also noted that the particle sizes distribution of the coexisting

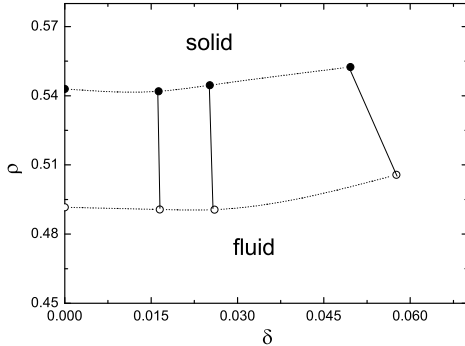


FIG. 4: The phase diagram of the polydisperse hard sphere system in the  $(\delta, \rho)$  plane. The dotted lines denote the boundaries of the fluid and solid phases. The solid lines denote the tie lines connecting the two coexisting phases.

solid differs from that of the prescribed target solid, this is because the volume of initial target solid is not equal to that of the coexisting solid, or we can determine directly the cloud points(the coexisting phase with a prescribed composition). Fig. 3 is the probability distribution of the volume at coexistence, the two equal height peaks of the distribution correspond to the coexisting fluid and solid phases, respectively. In Fig 4, we plot the phase diagram of the polydisperse HSS in the  $(\rho, \delta)$  plane. For the polydispersity used in the simulation, the phase diagram has the same properties as the previous simulation [3]. The transition points reported here are not accurately located because extensive runs are needed to refine the locations, but it is suffice to exhibit the validity of our method.

To conclude we provide a new Monte Carlo method to study the fluid-solid phase transition of the polydisperse colloidal system. The validity of the method is demonstrated by locating the fluid-solid transition point of the polydisperse HHS. The obtained results are consistent with the previous results. The method can be directly extended to the polydisperse soft-interaction systems and the hard-interaction system with other polydisperse attributes. It presents a complement to the current Gibbs-Duhem integration method [3]. The estimate of cloud points is important to fully understand the phase behavior of polydisperse colloids [30]. It is possible to extend our current method to determine the cloud points for the fluid-solid transition of a polydisperse system. We are working on this direction and the results will be reported in the near future.

The work is supported by the National Natural Science Foundation of China under grant No.10334020 and in part by the National Minister of Education Program for Changjiang Scholars and Innovative Research Team in University.

---

- [1] W.G. Hoover and F. H. Ree, *J. Chem. Phys.* 49, 3609 (1968).
- [2] P. N. Pusey and W. van Megen, *Nature (London)* 320, 340 (1986).
- [3] P.G. Bolhuis and D. A. Kofke, *Phys. Rev. E* 54, 634 (1996); *ibid* 59, 618 (1999).
- [4] M. Fasolo and P. Sollich, *Phys. Rev. Lett.* 91, 068301 (2003).
- [5] S. Phan, W. B. Russel, J. Zhu and P. M. Chaikin, *J. Chem. Phys.* 108, 9789 (1998).
- [6] S. Martin, G. Bryant, and W. van Megen, *Phys. Rev. E* 67, 061405 (2003).
- [7] H. J. Schope, G. Bryant and W. van Megen, *Phys. Rev. Lett.* 96, 175701 (2006).
- [8] R. McRae and A. D. J. Haymet, *J. Chem. Phys.* 88, 1114 (1988).
- [9] P. Chaudhuri, S. Karmakar, C. Dasgupta, H. R. Krishnamurthy, and A. K. Sood, *Phys. Rev. Lett.* 95, 248301 (2005).
- [10] R. P. Sear, *Europhys. Lett.* 44, 531 (1998).
- [11] P. Bartlett, *J. Chem. Phys.* 109, 10 970 (1998).
- [12] P. Bartlett and P. B. Warren, *Phys. Rev. Lett.* 82, 1979 (1999).
- [13] R. M. L. Evans and C. B. Holmes, *Phys. Rev. E* 64, 011404 (2001).
- [14] S. Auer and D. Frenkel, *Nature (London)* 413, 711 (2001).
- [15] N.B. Wilding and P. Sollich, *Europhys. Lett.* 67, 219 (2004)
- [16] L. A. Fernández, V. Martín-Mayor, and P. Verrocchio, *Phys. Rev. Lett.* 98, 085702 (2007).
- [17] M. A. Bates and D. Frenkel, *J. Chem. Phys.* 110, 6553 (1999).
- [18] M. C. Yang and H. R. Ma, *J. Chem. Phys.* 128, 134510 (2008).
- [19] N. B. Wilding and A. D. Bruce, *Phys. Rev. Lett.* 85, 5138 (2000).
- [20] D. Frenkel and A. J. C. Ladd, *J. Chem. Phys.* 81, 3188 (1984).
- [21] D. Frenkel and B. Smit, *Understanding Molecular Simulation* (Academic, San Diego, 1996).
- [22] C. Borgs and R. Kotecký, *J. Stat. Phys.* 61, 79 (1990); *Phys. Rev. Lett.* 68, 1734 (1992).
- [23] M. S. S. Challa, D. P. Landau and K. Binder, *Phys. Rev. B.* 34, 1841 (1986).
- [24] B. A. Berg and T. Neuhaus, *Phys. Rev. Lett.* 68, 9 (1992).
- [25] F. Wang, D. P. Landau, *Phys. Rev. Lett.* 86, 2050 (2001); *Phys. Rev. E* 64, 056101 (2001).

- [26] J. S. Wang and R. H. Swendsen, *J. Stat. Phys.* 106, 245 (2002).
- [27] N. B. Wilding, *J. Chem. Phys.* 119, 12163 (2003).
- [28] M. C. Yang and H. R. Ma, (unpublished).
- [29] M. Fasolo and P. Sollich, *Phys. Rev. E* 70, 041410 (2004).
- [30] M. Buzzacchi, P. Sollich, N. B. Wilding and M. Müller, *Phys. Rev. E* 73, 046110 (2006).